Desalination and Water Treatment
www.deswater.com

doi: 10.5004/dwt.2021.27218

225 (2021) 392–401
June

Determination of heat and mass transfer coefficients in a spray humidifier of a humidification–dehumidification desalination system

Karima Hijjaji[a,*], Slimane Gabsi[b], Nader Frikha[c]

[a]*Research Laboratory: Energy, Water, Environment & Processes LEEP (LR18ES35), National School of Engineers of Gabes, Gabès University, Street Omar Ibn ElKhattab – 6029 Gabès, Tunisia, email: karimahijjaji@gmail.com*
[b]*National School of Engineers of Sfax, 3038 Sfax, Sfax University, Tunisia*
[c]*Higher Institute of Biotechnology, Street Soukra BP 1175, 3038 Sfax, Sfax University, Tunisia*

Received 24 January 2020; Accepted 8 March 2021

ABSTRACT

An innovative design approach consists of using a saline water spray humidifier to improve the performance of the humidification–dehumidification water desalination system, where hot water was sprayed from the top and air was supplied from the bottom of the humidifier. Before scaling a unit of this type, it is necessary to get sufficient information about the heat and mass transfer process that occurs in the unit. A prototype desalination unit has been developed and used to fulfill the main objective of this research which is to evaluate the mass and heat transfer coefficients in the humidifier. As well, the effect of salt water flow rate, water temperature, air flow rate and position of the water spray are examined in order to optimize the operating conditions. A quadratic model estimating the performance of the humidifier was developed and validated using the design of experiment analysis and variance approach. A response surface methodology was used to correlate and assess the influence of each parameter and its interactions with the others. The results indicate that the effect of air flow rate and inlet water temperature on mass and heat transfer is greater than the height of the sprayer and the saline water flow rate. Binary interaction effects of the variables were taken into account and provided for the design recommendations.

Keywords: Desalination; Humidification–dehumidification; Sprayed water; Mass and heat transfer; Design of experiment

1. Introduction

By the year 2025, over 60% of the world's population will be confronted with water scarcity problems [1]. Water desalination is one of the main options to overcome this problem. However, the cost of fossil fuels and their effects on the environment are two major concerns that need to be taken into account for the development of these systems. In the aim of preserving the ecosystem by minimizing environmental impacts, desalination using renewable sources of energy seems to be a major challenge in this domain. Today, solar desalination has become a sustainable and affordable option to overcome freshwater stress, in particular in remote areas where solar radiation is very abundant. Several desalination processes are commonly used to provide fresh water, including multi-stage flash distillation, multi-effect distillation, vapor compression and reverse osmosis. However, the high energy consumption and high maintenance costs of these technologies make small-scale production of fresh water not economical [2]. For small-scale decentralized demand, one of the simplest and most efficient desalination processes is the humidification–dehumidification (HDH) process, which has such

* Corresponding author.

distinctive advantages as reduced energy consumption and the feasibility of operating with solar thermal energy at low temperatures [3]. All present humidification and dehumidification technologies for water desalination have very low capacity [4]; caused by the limited humidification of the air in the humidifier. Air humidification is carried out well below the saturation point, which results in lower fresh water yield at the end of dehumidification.

Niroomand et al. [5] investigates a HDH unit with a packed humidifier and a direct contact dehumidifier the sections of humidifier and dehumidifier were equal to 1 m × 1 m cross section area and 0.5 m height. The water was sprayed in cross flow with the air, the water droplets fall in a vertical direction however the air pass through the cross section. The mass and heat transfer coefficients in humidifier are analyzed. It was concluded that the water droplets diameter and initial velocity are the most influencing design parameters and must be very carefully chosen.

An overall optimization of the HDH process has been carried out by Soufari et al. [6]. The effects of different parameters were analyzed and a mathematical model was presented to optimize the process with different goal functions. Then, the model was developed by adding the solar part and finally a low-cost design for HDH desalination was obtained [7]. Based on the results of the optimization, a unit with a capacity of 10 L/h was built in the next step [8]. An indirect condenser is used as a dehumidifier, which preheats the salt water supply.

Raj et al. [9] studied an HDH desalination unit with a honeycomb packed humidifier. Warm salt water was sprayed from the top and air was supplied from the bottom, the effect of operational parameters such as water temperature, air and water mass flow were evaluated, performance parameters such as mass and heat transfer rate, range, evaporation rate, efficiency were calculated. They found that the maximum efficiency of the humidifier is 0.75 an air flow rate of 0.55 m^3/s and a water flow rate of 150 L/h.

Morales and Carvajal [10] presented a thermodynamic model analysis of a direct surface contact humidifier in an HDH system. A parametric study was performed to investigate the effects of mass flow and inlet temperature of air and seawater. It is found that both increasing the seawater mass flow rate and inlet temperature, the evaporation rate increases, and the relationship between air and seawater mass flow rates and the cross-sectional area of the humidifier are relevant for optimal design.

For studying the influence of different parameters and their interactions, response surface methodology (RSM) has been successfully employed by Rejeb et al. [11]. The findings indicated that the most influencing parameters on the amount of distilled water are ambient temperature, water depth, solar radiation, and thickness of insulation.

The current work is aimed at developing a new process to improve the water spray humidification process that increases the contact area of water with air and the heat and mass transfer. Laboratory-scale experiments have been conducted. The purpose of these experiments was to determine the heat and mass transfer coefficients in order to study the influence of operating conditions such as air flow rate, water flow rate, water temperature and spray height on the heat and mass transfer performance of the spray humidifier and to develop a correlation based on these parameters. A design of experiment (DOE) procedure was used to evaluate and correlate the effects of these parameters and their interactions. The results of this study will contribute to the design of a new solar desalination system.

2. Theoretical consideration

2.1. Heat and mass transfer coefficients calculation

The heat and mass transfer coefficients between air and water in the spray humidifier are calculated from the experimental data and heat and mass transfer balances.

The heat transfer coefficient of sensible-heat transfer between the air and water is calculated using the following relation [12]:

$$h_G = \frac{Q_a C_{\mathrm{Pa}} \left(T_{\mathrm{in}} - T_{\mathrm{out}}\right)}{\mathrm{H.P.LMTD}} \tag{1}$$

$$\mathrm{LMTD} = \frac{\left(\Delta T_1 - \Delta T_2\right)}{\ln\left(\frac{\Delta T_1}{\Delta T_2}\right)} \tag{2}$$

With $\Delta T_1 = T_e - T_{\mathrm{out}}$ and $\Delta T_2 = T_e - T_{\mathrm{in}}$.

The mass transfer coefficient between the air and water is calculated using the following relation [12]:

$$k_{\mathrm{mG}} = \frac{Q_a \left(Y_{\mathrm{in}} - Y_{\mathrm{out}}\right)}{\mathrm{H.P.LMHD}} \tag{3}$$

$$\mathrm{LMHD} = \frac{\left(\Delta Y_1 - \Delta Y_2\right)}{\ln\left(\frac{\Delta Y_1}{\Delta Y_2}\right)} \tag{4}$$

With $\Delta Y_1 = Y_e - Y_{\mathrm{out}}$ and $\Delta Y_2 = Y_e - Y_{\mathrm{in}}$.

2.2. Physical properties of humid air

The following expressions were used for calculating values of the physical properties of air:

$$Y = \frac{m_v}{m_a} = 0.622 \frac{\varphi P_{\mathrm{vs}}}{P_t - \varphi P_{\mathrm{vs}}} \tag{5}$$

$$Y_e = 0.622 \frac{\left(1 \cdot P_{\mathrm{vs}}\right)}{P_t - 1 \cdot P_{\mathrm{vs}}} \tag{6}$$

$$P_{\mathrm{vs}} = \exp\left(13{,}765 - \frac{5{,}123}{T + 273.15}\right) \tag{7}$$

$$C_{\mathrm{Pa}} = 4{,}185\left[0.24\left(1 - Y_a\right) + 0.46 Y_a\right] \tag{8}$$

$$\rho_a = \frac{357{,}57 \times 10^{-5}}{\left(T + 273.15\right)}\left(P_t - 0.378 P_v\right) \tag{9}$$

$$P_v = P_{vs}\varphi\left(P_a\right) \tag{10}$$

3. Materials and methods

3.1. Experimentation

The experimental device is run as a cycle that begins with the recirculation of brackish water by a centrifugal pump coupled to a sprayer; the water is preheated in a water bath attached to a humidifier made of Plexiglas having a length of 30 cm, width of 30 cm, and height of 90 cm. At this level the humidification of the dry air is started by injecting it into the humidifier using a compressor. When the water heats up until it evaporates, the steam produced will be transported to the condensation tower as moist air. The water used in this study is real brackish water with a salinity of 8.16 g/L.

On a global point of view, we can consider that this desalination system consists of two interacting circuits: the saline water circuit and the atmospheric air circuit. This interaction is driven by the heat and mass transfer actual mechanisms.

Fig. 1 shows the schematic diagram of the experimental setup.

3.2. Data acquisition system

For the measurement of the humidity and the temperature, a digital hygro-thermometer (CA1244) that ranges from 0 to 100% RH and from −40 to +120°C with an uncertainty of 1.1%. The psychrometric air properties are computed by Computer-Aided Thermodynamic Table software.

The air flow rate was measured using a rotameter with a range of 0–10 $Nm^3/$.

The water flowrate was measured using a rotameter with a range of 0–600 L/h.

The measurement are performed on the steady state conditions that are, due mainly to the thermal inertial effects, reached roughly after 30 min depending on the ambient conditions that drives the air inlet temperature and the heat transfers between the still and the external environment.

4. Design of experiments

To obtain a general analytic model for the desalination productivity of the proposed system as a function of the main design and functioning parameter, the DOE procedure is applied. RSM [13] is used for modeling, and analyzing this problem that involves multiple variables influencing the response. A second-order regression model is used in RSM as it provides numerous advantages among which its versatility that allows it to fit more closely the true response surface of the system [14].

In the DOE, the involved factorial procedure allows the experiment to be conducted under all possible combinations of the parameters set at different levels. A design matrix is set up with these combinations where the rows represent the trials and the columns represent their levels.

Four a priori influencing parameters have been chosen in this work based on a preliminary study: the air and the water flow rates, the saline water temperature and the height of the sprayers. The last parameter represents the height of the saline water sprayers accounted from the water basin surface. Three levels have been chosen for each parameter as presented in Table 1. Notice that the inlet air temperature was no more been heated in this study. In fact, heating the salt water is easier, and also cheaper due to the heat exchangers size which had to achieve successive heating operation of water or air.

The design matrix row and column are shown in Table 2 of the studied solar still. There are three-level central composite rotatable designs consisting of 21 sets of coded

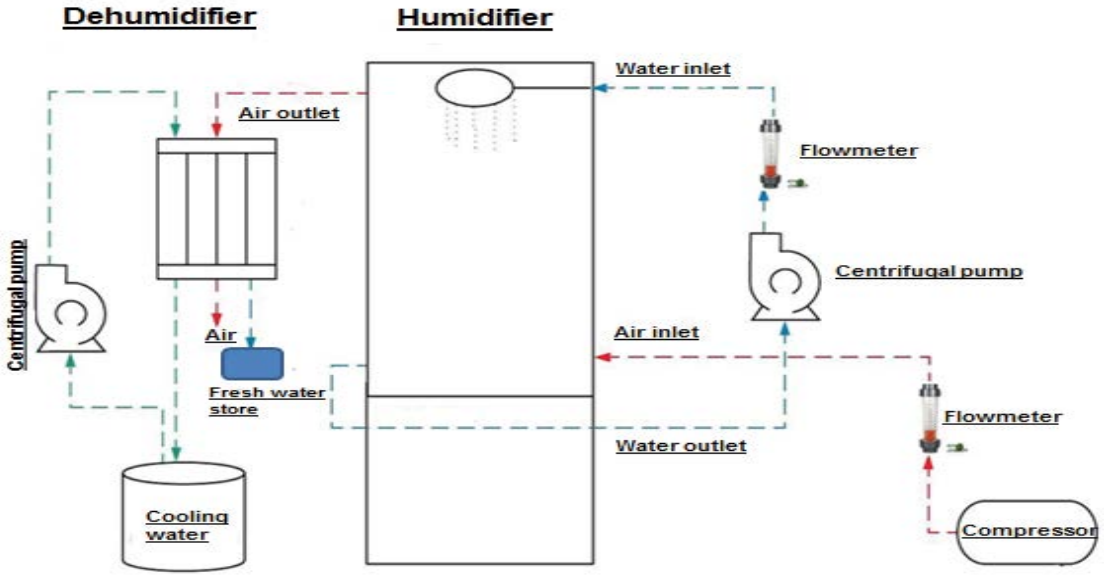

Fig. 1. Schematic diagram of the humidification–dehumidification desalination system.

conditions composed of a full factorial $2^4 = 16$ plus 5 centre points,

As there are only three levels for each factor, the appropriate model is the quadratic model [15].

$$Y = \beta_0 + \sum_{i=1}^{k}\beta_i x_i + \sum_{i=1}^{k}\beta_{ii}x_i^2 + \sum_{i=1}^{k-1}\sum_{j=2(i\neq j)}^{k}\beta_{ij}x_i x_j + \varepsilon \quad (11)$$

where Y is the response; x_i and x_j are the variables; β_0 is a constant coefficient; β_i, β_{ii}, and β_{ij} are the interaction coefficients of linear, quadratic, and second-order terms, respectively; k is the number of studied factors; and ε is the error. The values of the coefficient in this equation were calculated by regression of the response surface with the help of DOE analysis in MINITAB software package. The insignificant coefficients were eliminated by the means of back elimination technique used to determine the significant coefficients. The final mathematical model was constructed using the significant coefficients [15].

Table 1
Parameters levels

Parameters	Factors	Factors levels		
		–1	0	1
Air mass flux, kg/m² h	Q_a	8.7	30.5	52.3
Water mass flux, kg/m² h	Q_w	266.4	999	1,731.6
Salt water temperature, °C	T_w	40	55	70
Spray height, m	H	0.4	0.6	0.8

5. Results and discussion

5.1. Parametric study

Prior to generate data for the statistical analysis, a parametric experimental investigation was conducted to study the influence of operating and design variables on the heat and mass transfer coefficient, and to determine the range of each variable.

5.1.1. Effect of the air mass flow on transfer coefficients

As shown in Fig. 2, the transfer coefficients rate increase advantageously with the air mass flow. The circulation of higher air volumetric flow improves the air-water heat and mass convective transfer rates, and leads, in the other hand, to less saturated air that permits higher diffusion mass transfer between the two fluids. It is clear that in an air humidification basin, the air flow rate is the parameter that has the most influence on the mass and heat transfer coefficients.

5.1.2. Effect of the water mass flow on transfer coefficients

The effect of sprayed water mass flow on mass and heat transfer coefficients is depicted in Fig. 3. As shown in this figure, by setting the air flow rate at 17.4 kg/m² h, the temperature at 50°C and when the regime is reached, the water flow rate ranges from 800 to 1,734 L/h. It can be seen that the mass and heat transfer coefficients increase as the flow rate of water spray increases. On the one hand the effect is important for the heat transfer coefficient h_G, indeed an increase of 800 to 1,734 L/h of water flow causes

Table 2
Experimentation matrix and experimental responses

Run	Q_a	Q_w	T_w	H	$k_m{\cdot}a$ (kg/m³ s atm)	$h_G{\cdot}a$ (W/m³ K atm)
1	–1	–1	–1	+1	6.19×10^{-3}	3.91
2	+1	–1	–1	+1	3.64×10^{-2}	16.47
3	–1	+1	–1	+1	7.66×10^{-3}	8.59
4	+1	+1	–1	+1	4.67×10^{-2}	36.26
5	–1	–1	+1	+1	6.51×10^{-3}	5.40
6	+1	–1	+1	+1	4.06×10^{-2}	23.25
7	–1	+1	+1	+1	8.14×10^{-3}	10.15
8	+1	+1	+1	+1	4.98×10^{-2}	44.80
9	–1	–1	–1	–1	9.84×10^{-3}	4.94
10	+1	–1	–1	–1	5.68×10^{-2}	22.92
11	–1	+1	–1	–1	9.63×10^{-3}	10.44
12	+1	+1	–1	–1	5.70×10^{-2}	46.78
13	–1	–1	+1	–1	1.02×10^{-2}	9.31
14	+1	–1	+1	–1	6.06×10^{-2}	41.59
15	–1	+1	+1	–1	1.31×10^{-2}	13.31
16	+1	+1	+1	–1	8.73×10^{-2}	62.89
17	0	0	0	0	4.02×10^{-2}	19.32
18	0	0	0	0	4.02×10^{-2}	19.25
19	0	0	0	0	3.99×10^{-2}	19.64
20	0	0	0	0	4.02×10^{-2}	19.37
21	0	0	0	0	4.00×10^{-2}	19.33

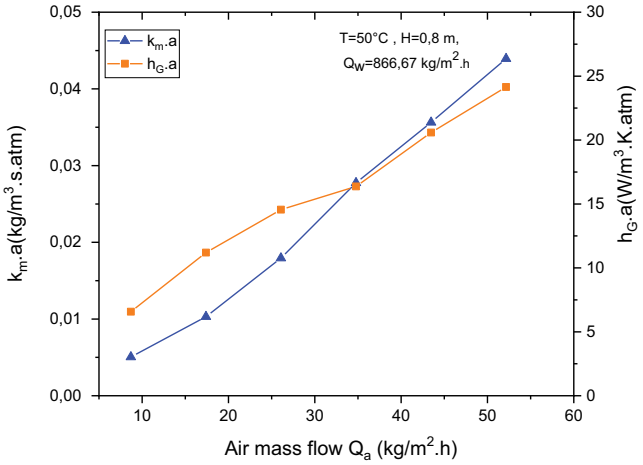

Fig. 2. Effect of the air mass flow on transfer coefficients.

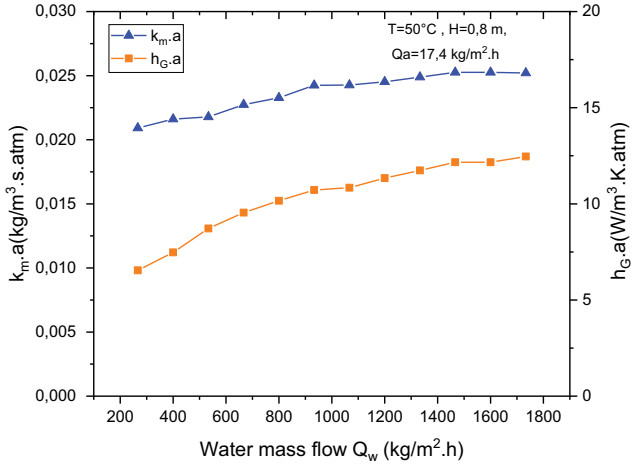

Fig. 3. Effect of the water mass flow on transfer coefficients.

a 100% increase of h_G and only a 14% increase of the material transfer coefficient k_m. The increase of the water flow rate leads to an increase in the number of droplets which generates more exchange surface. In addition, the increase in velocity and turbulence increases with the increase in water flow which favors the increase in transfer coefficients.

5.1.3. Effect of the saline water temperature on transfer coefficients

The effect of the sprayed water temperature on the productivity is depicted in Fig. 4. During this study the temperature will be varied between 40°C and 70°C. This temperature is regulated with the help of the thermostat bath which is equipped with two thermal heaters ensuring the heating of the water. It can be seen that the water temperature has a greater influence on the heat transfer coefficient than on the mass transfer coefficient; in fact we notice a greater increase in the heat transfer coefficient h_G when the water temperature rises. The variation from 40°C to 50°C temperature causes a 10% increase in k_m and above 50°C k_m becomes almost constant. This is explained by the fact that increasing the water

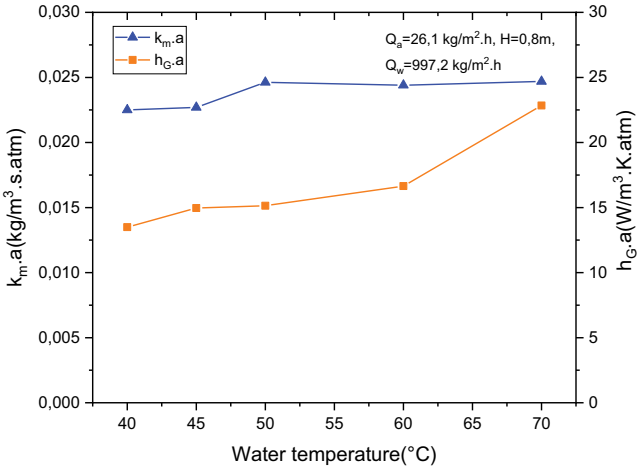

Fig. 4. Effect of the saline water temperature on transfer coefficients.

temperature leads to increasing the surrounding air temperature and consequently decreases its relative humidity because the capacity of the air to humidify increases with temperature. It can be concluded that increasing the water temperature improves the transfer coefficients.

5.1.4. Effect of the spray height on transfer coefficients

To study the effect of the height of the sprayer, the air flow rate is set at 52.3 kg/m² h, the water flow rate at 1,731.6 kg/m² h and the temperature is set at 70°C while varying the height at 3 levels (0.4, 0.6 and 0.8 m). Fig. 5 shows the variation of transfer coefficients versus sprayer height. It shows that an increase in sprayer height causes a decrease in transfer coefficients. This is explained by the fact that the h_G is inversely proportional to the sprayer height. The water droplet diameter reduction during the falling time may also play a role since the heat and mass transfer are enhanced as a consequence of the droplet diameter reduction. One can notice that as the column height increases there is a trend decrease of the mass and heat transfer coefficient increasing with the column height increasing. That is due to more air humidity saturation.

5.2. Statistical analysis and modeling

After making sure of the accuracy of mathematical model, we have to study the sensitivity of variable parameters effective on transfer coefficients through DOE analysis.

Based on the general model set up by Eq. (6) and the experimental study on the designed solar still conducted under the DOE procedure, the parameters β_0, β_i, β_{ii} and β_{ij} have been computed and Eq. (11) led to Eqs. (12) and (13). The equations obtained are:

$$k_m \cdot a = 10^{-3}\begin{pmatrix} -6.9 + 2.221Q_a - 0.00040Q_w - 0.023T_W \\ +0.4H - 0.01777Q_a{}^2 + 0.000159Q_a \times Q_w \\ +0.00699Q_a \times \mathrm{Tw} - 1.060Q_a \times H \end{pmatrix} \quad (12)$$

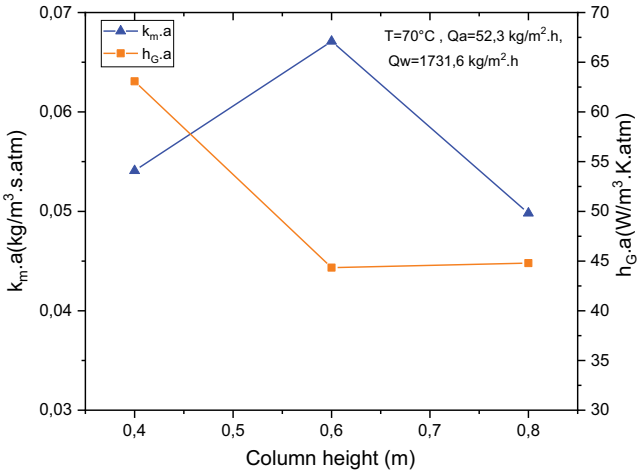

Fig. 5. Effect of the spray height on transfer coefficients.

$$h_g \cdot a = -12.20 - 0.060Q_a + 0.000923Q_w + 0.3152T_w + 26.32H + 0.00668Q_a^{\,2} + 0.000264Q_a \times Q_w + 0.00760Q_a \times T_W - 0.6228Q_a \times H - 0,493T_w \times H \quad (13)$$

To assess the robustness of the model, graphical comparisons were made with the experimental results to show the trend in the data. The predicted results and experimental data for mass and heat transfer coefficients are presented in Fig. 6. This comparison shows that the correlations obtained from Eqs. (12) and (13) are a highly successful tool for the prediction of experimental data.

The values of R^2 and adjusted R^2 are given in Table 3. The R^2 value were 0.973 and 0.996; which indicates that only 2.7% of the different variations for the mass transfer coefficient and 0.4% for the heat transfer coefficient were not explained by the model. This high value of R^2 reflects the excellent correlation between the independent variables and the response. The adjusted coefficient of variation R^2_{adjust} (0.955, 0.993) demonstrates the high precision and the consistence of the approved experiments.

Table 3
Model verification coefficients

Coefficient	R^2	R^2 (adjust)
k_{mG}	97.32%	95.54%
h_G	99.61%	99.30%

The robustness of our model was also verified using the analysis of variance technique (Table 4). The *F*-value from Fisher's law is a decisive indicator for the assessment of the experimental data [16]. The model's *F*-value in this analysis was calculated to be 54.51 for k_m and 315.98 for h_G and is associated with weak *P*-value ($P < 0.0001$). This association of the *F*-value and the low *P*-value reveals that the model is statistically significant in predicting mass and heat transfer coefficients. Thus, a *P*-values less than 0.05 indicate a significant model term, while values greater than 0.1 signal an insignificant model term [17]. Such a mathematical statistical approach indicates that the model and the model terms are a strongly significant model and the regression equation explains the major variations in response.

5.3. Interaction effects

The four parameter interactions, transfer coefficients can be plotted based on Eqs. (12) and (13). These interaction contours plot presented in Figs. 7 and 8 are a useful tool to show the simultaneous effect of each

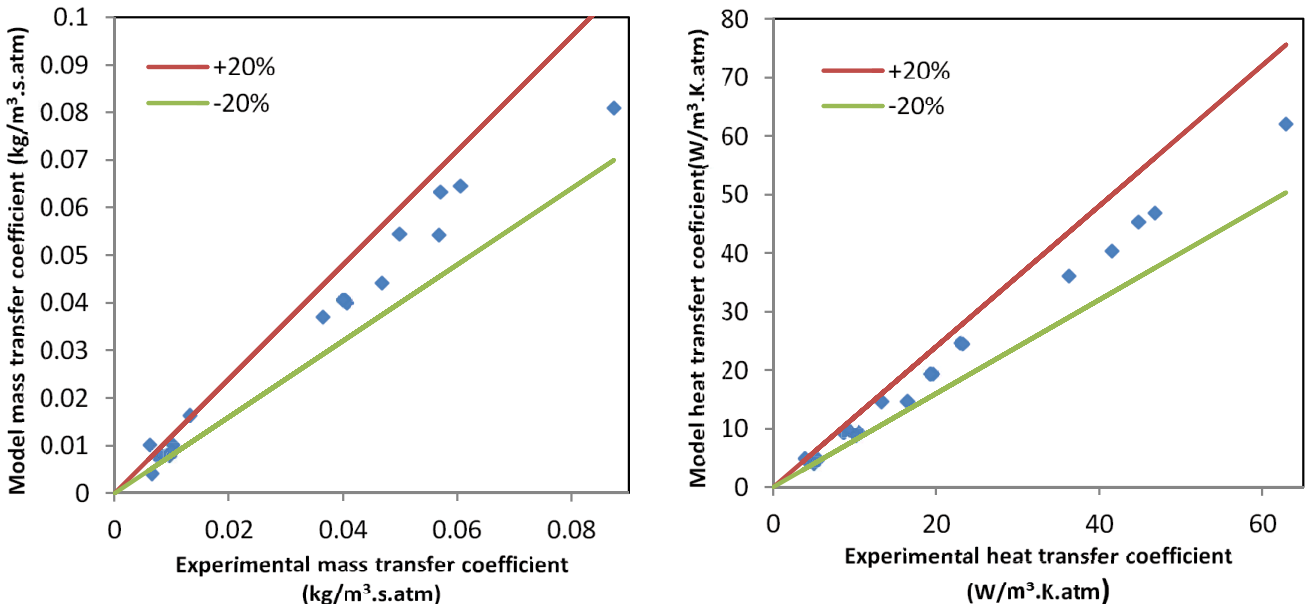

Fig. 6. Comparison of predicted mass and heat transfer coefficients with experimental results.

Table 4
Variance analysis

- Mass transfer coefficient

Source	DF	Adj. SS	Adj. MS	*F*-value	*P*-value
Model	8	10,047.4	1,255.92	54.51	0.000
Linear	4	9,245.7	2,311.43	100.33	0.000
Q_a	1	8,287.7	8,287.69	359.72	0.000
Q_w	1	171.2	171.17	7.43	0.018
T_w	1	130.8	130.82	5.68	0.035
H	1	656.0	656.04	28.47	0.000
Square	1	272.0	272.01	11.81	0.005
Q_a^2	1	272.0	272.01	11.81	0.005
2-way interaction	3	529.7	176.56	7.66	0.004
$Q_a \times Q_w$	1	103.7	103.65	4.50	0.055
$Q_a \times T_w$	1	83.7	83.75	3.64	0.081
$Q_a \times H$	1	342.3	342.27	14.86	0.002
Error	12	276.5	23.04		
Lack-of-fit	8	276.4	34.55	1,654.44	0.000
Pure error	4	0.1	0.02		
Total	20	10,323.9			

- Heat transfer coefficient

Source	DF	Adj. SS	Adj. MS	*F*-value	*P*-value
Model	9	5,024.41	558.27	315.98	0.000
Linear	4	4,448.56	1,112.14	629.47	0.000
Q_a	1	3,274.91	3,274.91	1,853.59	0.000
Q_w	1	694.73	694.73	393.22	0.000
T_w	1	227.95	227.95	129.02	0.000
H	1	250.98	250.98	142.05	0.000
Square	1	38.46	38.46	21.77	0.001
Q_a^2	1	38.46	38.46	21.77	0.001
2-way interaction	4	537.39	134.35	76.04	0.000
$Q_a \times Q_w$	1	285.40	285.40	161.54	0.000
$Q_a \times T_w$	1	98.96	98.96	56.01	0.000
$Q_a \times H$	1	118.06	118.06	66.82	0.000
$T_w \times H$	1	34.97	34.97	19.79	0.001
Error	11	19.43	1.77		
Lack-of-fit	7	19.34	2.76	120.29	0.000
Pure error	4	0.09	0.02		
Total	20	5,043.84			

parameter and their mutual interactions as the effect of one factor depends on the level of each other.

5.3.1. Effect of Q_w and Q_a

It appears that the mass transfer coefficient reaches its maximum for the highest air flow rate and highest water flow rate. Besides, the heat transfer coefficient increases as the mass flow rates of the both fluids increase. However, the effect of air flow rate is most significant, then for a low air mass flow; there is no significant improvement in the mass and heat transfer coefficient by increasing the water flow rate, due to a lower performance improvement when the air becomes saturated.

5.3.2. Effect of Q_a and T_w

Shows the simultaneous variations in air mass flow and water temperature. It is clear that the heat and the mass transfer coefficients increase in a high ratio with an increase in both the water temperature and the air flow rate. However, this increasing ratio is more

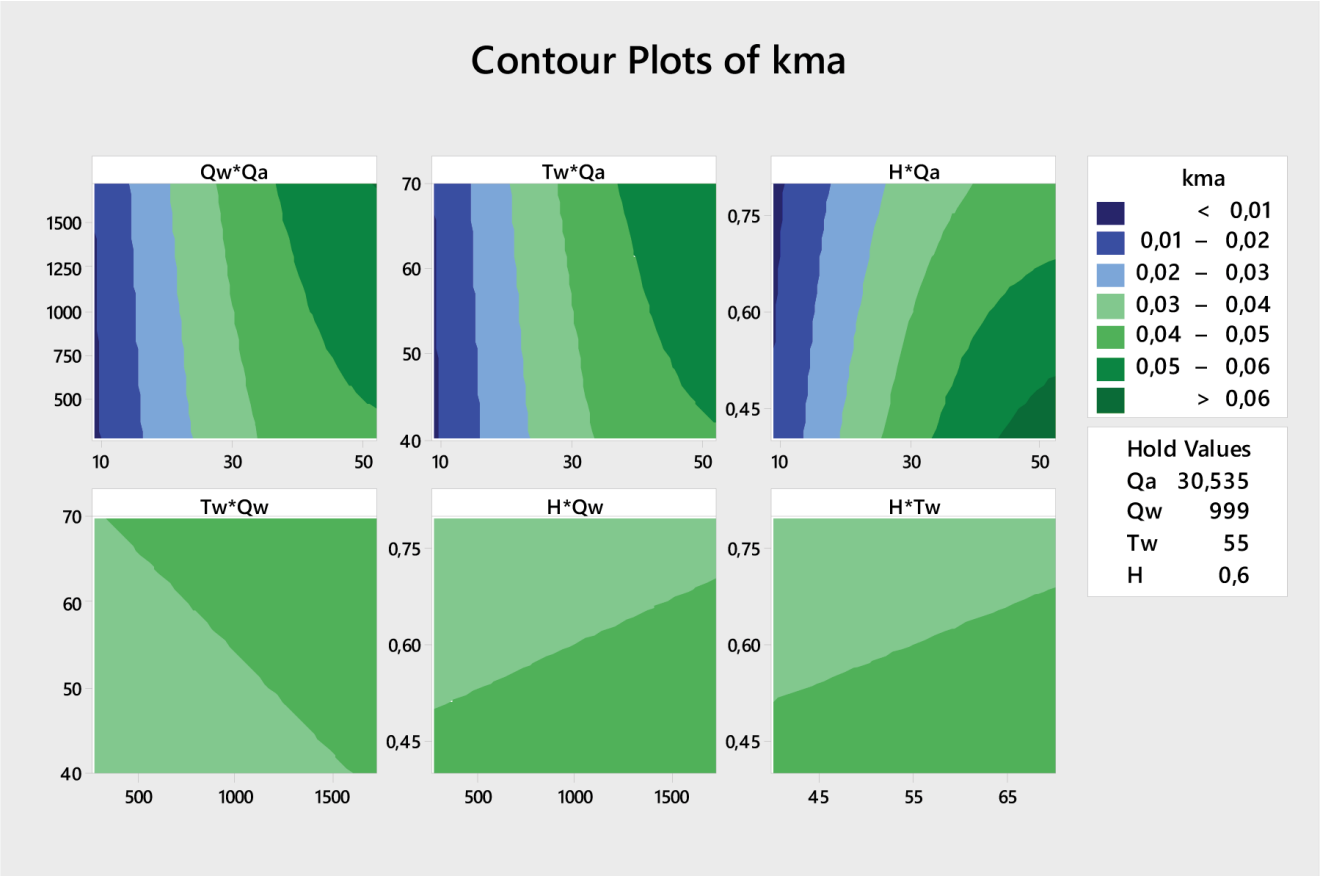

Fig. 7. Contours plots of mass transfer coefficient as a function of: Q_w × Q_a (water flow rate and air flow rate); T_w × Q_a (water temperature and air flow rate; H × Q_a (spray height and air flow rate); (T_w × Q_w) temperature and water flow rate; (H × Q_w) spray height and water flow rate; H × T_w (spray height and water temperature).

important at high water temperature. Thus, a low air mass flow is recommended for low water temperatures to reduce the ventilation power consumption.

5.3.3. Effect of Q_a and H

It presents the effect of the air mass flow on the system productivity at different column height. The heat and the mass transfers increase with an increase in the air flow rate and a decrease in the height of sprayer and the effect of spray height is relatively less than the one of the air mass flow.

5.3.4. Effect of T_w and Q_w

The contour interaction of the sprayed water flow and the water temperature indicates that the both transfer coefficients are slightly affected by the sprayed water flow rate for lower water temperatures. However it is more significant for higher temperatures. So, an appropriate water mass flow had to be chosen according to the water temperature to reduce the pumping cost.

5.3.5. Effect of H and Q_w

The interaction between the height of sprayer and water flow rate do not have any considerable effect on mass and heat transfer coefficients. It is observed that the increase of the water mass flow rate and the decrease of sprayer height increases the water evaporated rate in a relative low ratio. One may conclude that for a low sprayer height, it is recommended to work with high water mass flow.

5.3.6. Effect of H and T_w

The effect of the interaction between the height of sprayer and water temperature on mass and heat transfer coefficients is less important negligible. It indicates that the increase of the sprayer height decreases the heat and mass transfer coefficient. However the effect of decreasing the sprayer height is more interesting for high water temperature values.

6. Conclusion

An experimental study was carried out to investigate the influence of various operating conditions on the efficiency of air humidification in a simple spray humidifier. Within the range of experimental conditions studied, humidity can reach almost 100%. The effect of air flow rate and saline water temperature are the most significant on mass and heat transfer.

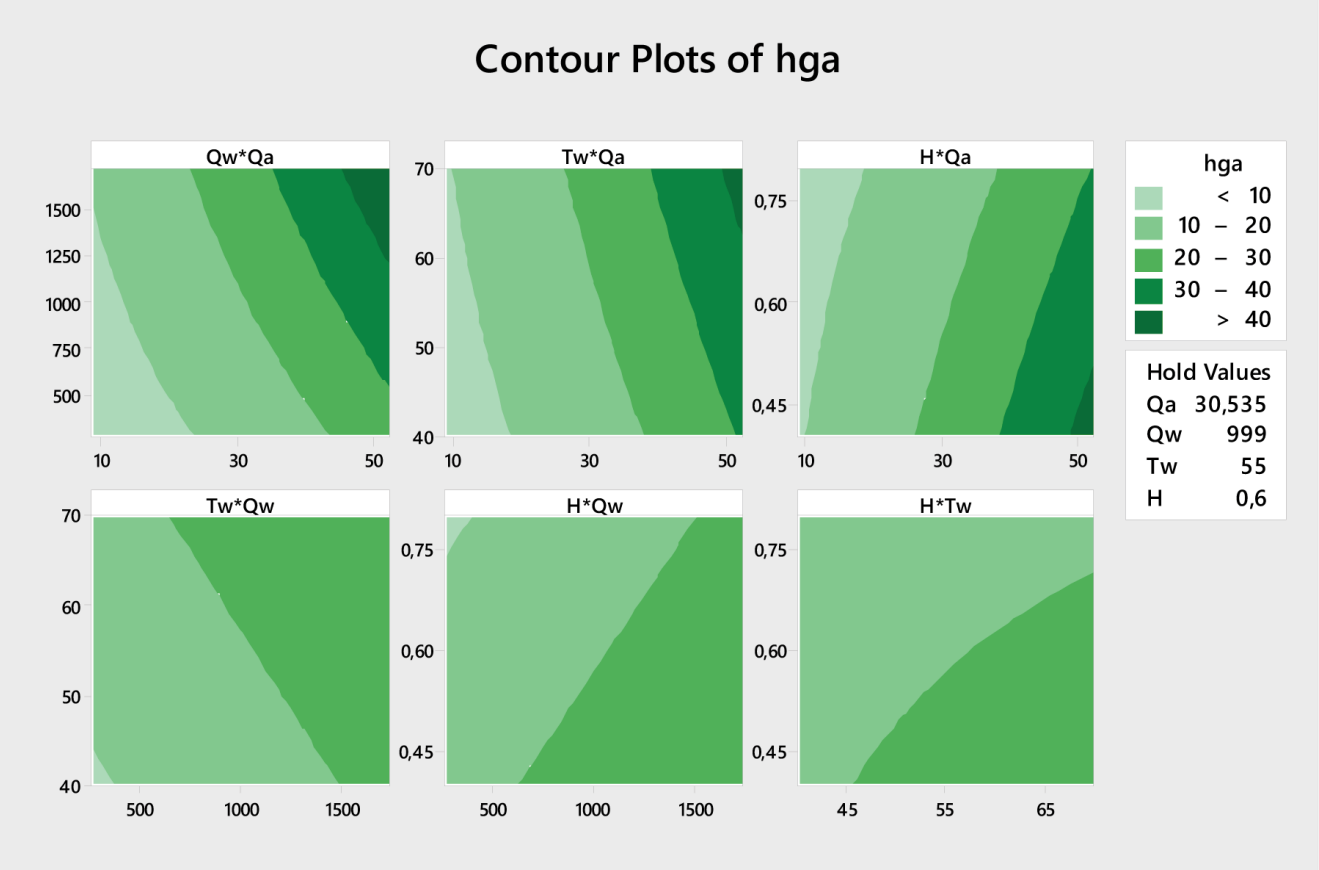

Fig. 8. Contours plots of heat transfer coefficient as a function of: $Q_w \times Q_a$ (water flow rate and air flow rate); $T_w \times Q_a$ (water temperature and air flow rate; $H \times Q_a$ (spray height and air flow rate); ($T_w \times Q_w$) temperature and water flow rate; ($H \times Q_w$) spray height and water flow rate; $H \times T_w$ (spray height and water temperature).

In this study, the mass and heat transfer coefficients in the humidifier were determined. With the developed models, the heat and mass transfer coefficients can be successfully predicted as a function of air flow rate, water flow rate, temperature and height of the humidifier.

This investigation will serve as a fundamental design tool for the building of a new desalination system.

Symbols

a	—	Specific gas–liquid interfacial area, m²/m³
C_p	—	Specific heat capacity, J/kg K
H	—	Spray height, m
$h_G \cdot a$	—	Heat transfer coefficient, W/m³ K atm
$k_m \cdot a$	—	Mass transfer coefficient, kg/s m³ atm
LMHD	—	Difference logarithmic mean humidity, kg/kg dry air
LMTD	—	Difference logarithmic mean temperature, °C
P_t	—	Total pressure, Pa
P_v	—	Vapor pressure, Pa
P_{vs}	—	Partial pressure, Pa
Q	—	Mass flow, kg/m² h
T	—	Temperature, °C or K
Y	—	Absolute humidity, kg/kg dry air
Y_e	—	Saturation humidity, kg/kg dry air

Greek

ρ	—	Density, kg/m³
φ	—	Relative humidity, %

Subscripts

a	—	Air
w	—	Water
in	—	Inlet
out	—	Outlet

References

[1] F.R. Zhang, Prediction of China's water shortage in the year of 2025, Appl. Mech. Mater., 409–410 (2013) 83–88.
[2] M.A. Sharaf, A.S. Nafey, L. García-Rodríguez, Thermo-economic analysis of solar thermal power cycles assisted MED-VC (multi effect distillation-vapor compression) desalination processes, Energy, 36 (2011) 2753–2764.
[3] H. Abd-ur-Rehman, F. Al-Sulaiman, Mathematical Modeling of Bubbler Humidifier for Humidification–Dehumidification (HDH) Water Desalination System, Proceedings of the 1st International Conference on Mechanical and Transportation Engineering, Kuala Lumpur, Malaysia, 2015.
[4] M.M. Alhazmy, Minimum work requirement for water production in humidification—dehumidification desalination cycle, Desalination, 214 (2007) 102–111.

[5] N.M. Niroomand, M. Zamen, M. Amidpour, Theoretical investigation of using a direct contact dehumidifier in humidification–dehumidification desalination unit based on an open air cycle, Desal. Water Treat., 54 (2015) 305–315.
[6] S.M. Soufari, M. Zamen, M. Amidpour, Performance optimization of the humidification–dehumidification desalination process using mathematical programming, Desalination, 237 (2009) 305–317.
[7] M. Zamen, M. Amidpour, S.M. Soufari, Cost optimization of a solar humidification–dehumidification desalination unit using mathematical programming, Desalination, 239 (2009) 92–99.
[8] S.M. Soufari, M. Zamen, M. Amidpour, Experimental validation of an optimized solar humidification–dehumidification desalination unit, Desal. Water Treat., 6 (2009) 244–251.
[9] A. Raj, R. Bajaj, T. Srinivas, Performance Evaluation of Honeycomb Structured PVC Packed Humidifier in a Humidification–Dehumidification Desalination Plant, 2016 International Conference on Energy Efficient Technologies for Sustainability (ICEETS), IEEE, Nagercoil, India, 2016.
[10] A.A. Morales, D.S. Carvajal, Heat and Mass Transfer in a Direct Contact Humidifier of a Humidification–Dehumidification Desalination System, 2017 IEEE 6th International Conference on Renewable Energy Research and Applications (ICRERA), IEEE, San Diego, CA, USA, 2017.
[11] O. Rejeb, M.S. Yousef, C. Ghenai, H. Hassan, M. Bettayeb, Investigation of a solar still behaviour using response surface methodology, Case Stud. Therm. Eng., 24 (2021) 100816, doi: 10.1016/j.csite.2020.100816.
[12] K.H. Javed, T. Mahmud, E. Purba, Enhancement of mass transfer in a spray tower using swirling gas flow, Chem. Eng. Res. Des., 84 (2006) 465–477.
[13] D.C. Montgomery, Design and Analysis of Experiments, John Wiley & Sons, Hoboken, NJ, 2017.
[14] R.H. Myers, D.C. Montgomery, C.M. Anderson-Cook, Response Surface Methodology: Process and Product Optimization Using Designed Experiments, John Wiley & Sons, Hoboken, NJ, 2016.
[15] L. Custer, D.R. McCarville, D.C. Montgomery, Student Solutions Manual to Accompany Design and Analysis of Experiments, John Wiley & Sons, New York, 2006.
[16] J. Antony, Design of Experiments for Engineers and Scientists, Elsevier, 2014.
[17] B.K. Körbahti, A. Tanyolaç, Electrochemical treatment of simulated textile wastewater with industrial components and Levafix Blue CA reactive dye: optimization through response surface methodology, J. Hazard. Mater., 151 (2008) 422–431.